# Formation and Movement of Myosin-containing Structures in Living Fibroblasts

**Nancy M. McKenna, Yu-li Wang, and Michael E. Konkel**

Cell Biology Group, Worcester Foundation for Experimental Biology, Shrewsbury, Massachusetts 01545

*Abstract.* Gizzard myosin, fluorescently labeled with tetramethylrhodamine iodoacetamide, was microinjected into living 3T3 fibroblasts to label myosin-containing structures. The fluorophore was located predominantly on the heavy chain near the COOH terminus of the S1 head and on the 17-kD light chain. After microinjection of a tracer amount into living 3T3 cells, the fluorescent myosin showed a distribution identical to that revealed by immunofluorescence with antimyosin antibodies. Injected myosin became localized in small beads, which were found along large stress fibers, along fine fibers, and in a poorly organized form near the lamellipodia. De novo assembly of beads was observed continuously within or near the lamellipodia, suggesting that myosin molecules may undergo a constant cycling between polymerized and unpolymerized states. The nascent structures then moved away from lamellipodia and became organized into linear arrays. Similar movement was also observed for beads already associated with linear structures, and may represent a continuous flux of myosin structures. The dynamic reorganization of myosin may play an important role in cell movement and polarity.

MYOSIN, one of the major structural components in muscle cells, is also present in most nonmuscle cells (for recent reviews see Warrick and Spudich, 1987; and Korn and Hammer, 1988; the discussion throughout this paper will be limited to myosin II). However, its precise roles in nonmuscle cells are still poorly understood. Although the organization of some nonmuscle myosin molecules, such as those along stress fibers, appears somewhat similar to the organization of myosin in muscle myofibrils (Langanger et al., 1986), there are important biochemical, structural, and possibly functional differences between myosins in muscle and nonmuscle cells.

One of the most important characteristics of nonmuscle myosin is its ability to undergo reorganization. For example, myosin molecules become concentrated in the contractile ring during cytokinesis (Fujiwara and Pollard, 1976). When cell surface receptors are induced to cap by ligands, myosin molecules co-cap with receptors and actin filaments (Bourguignon and Singer, 1977). In addition, when the slime mold *Dictyostelium* is stimulated by cAMP, myosin molecules relocate from the inner cytoplasm onto the cortex (Yumura and Fukui, 1985).

Several factors may contribute to the dynamic behavior of nonmuscle myosin molecules. First, the assembly of smooth muscle and nonmuscle myosins in vitro can be regulated by the phosphorylation of light or heavy chains (Warrick and Spudich, 1987; Korn and Hammer, 1988). Possible roles of phosphorylation in vivo are suggested by the increase in phosphorylation upon cellular activation (Warrick and Spudich, 1987; Korn and Hammer, 1988), and by the disruption of myosin-containing structures following inhibition of the light chain kinase (Lamb et al., 1988). The ability to regulate assembly also implies that there may be a pool of unassembled myosin in the cell. Second, the structures formed by nonmuscle myosin may be smaller, less well organized, and less stable than skeletal muscle thick filaments. In *Dictyostelium*, the predominant form of myosin appears to be a network of short rods (Yumura and Fukui, 1985). Short bipolar filaments were also identified along stress fibers of fibroblasts (Langanger et al., 1986). Third, it is also possible that myosin-containing structures may be able to move in nonmuscle cells. The ability of myosin-coated particles to move along actin filaments in cell models has been demonstrated (Sheetz and Spudich, 1983). If myosin-containing structures are not anchored in living cells, they may also undergo active movement in the cytoplasm.

So far the dynamics of myosin have only been deduced based on stationary images of fixed cells. However, in order to understand the process, it is crucial to make direct observations on living cells and answer questions such as when and where the assembly of myosin filaments takes place, and whether existing filaments move and reorganize in the cytoplasm. In the present study, we examine these questions by microinjecting fluorescently labeled smooth muscle myosin into living 3T3 fibroblasts. The fluorescent conjugate became incorporated into physiological structures, which appeared to consist of bead-like units. Using a low light level video camera and digital image processing, we were able to observe the de novo assembly of these beads near the lamellipodia, the movement of the beads away from the lamellipodia, and

the organization of beads into linear arrays. These activities, coupled to a possible dynamic exchange of myosin molecules between assembled and unassembled forms, may play an important role in cell polarity and/or motility.

## Materials and Methods

### Preparation of Proteins

Alpha actinin was prepared and fluorescently labeled with 5-iodoacetamidofluorescein as described previously (Meigs and Wang, 1986). Myosin was prepared from turkey gizzards according to Kendrick-Jones et al. (1983), or to Ikebe and Hartshorne (1985). Its purity was confirmed by SDS gel electrophoresis (Fig. 1). Purified myosin was stored either as a precipitate in 70% ammonium sulfate at 4°C, or as synthetic filaments at a low ionic strength in liquid nitrogen.

Myosin was labeled with tetramethylrhodamine iodoacetamide (Molecular Probes, Inc., Eugene, OR). The dye was dissolved in a labeling buffer of 500 mM KCl, 50 mM Hepes, pH 8.0, at a concentration of 0.3 mg/ml and clarified by centrifugation at 100,000 *g* for 15 min. The absorbance of the supernatant was measured and an appropriate volume (in milliliters), calculated as (1.4/absorbance) × milligrams of myosin, was mixed with myosin in the same buffer at a concentration of 8 mg/ml. After reacting for 2 h on ice, the solution was passed through a Bio-Bead SM-2 (Bio-Rad Laboratories, Richmond, CA; Meigs and Wang, 1986) column to remove unconjugated dye. Fluorescent fractions were pooled and dialyzed against 20 mM KCl, 20 mM Hepes, pH 7.5, for 5–15 h. Precipitated myosin was then collected by centrifugation, resuspended in an injection buffer of 450 mM KCl, 2 mM Pipes, pH 7.0, and dialyzed against the same buffer. The solution was clarified in a rotor (type 42.2Ti; Beckman Instruments, Inc., Palo Alto, CA) at 25,000 rpm (76,000 *g*) for 20 min, and was used for microinjection within 48 h.

The conjugate was free of noncovalently associated dye, which moves ahead of the tracking dye in a SDS-polyacrylamide gel. Most experiments were performed with myosin labeled at a ratio of 3.7 to 4.2, estimated based on a molar extinction coefficient of 47,000 at 555 nm for bound tetramethylrhodamine (DeBiasio et al., 1988). The results were not affected by the extent of labeling.

### Characterization of Myosin

Urea-glycerol gel electrophoresis was used to confirm that the 20-kD light chain of myosin was unphosphorylated (Perrie and Perry, 1970). Light chains prepared from thiophosphorylated myofibrils were used as the standard. Limited proteolytic digestion was performed by incubating 7.5 mg/ml myosin in 500 mM KCl, 0.1 mM EDTA, 10 mM Hepes, pH 7.5, with 10 μg/ml papain (Cooper Biomedical, Inc., Malvern, PA; activated in 50 mM cysteine at 37°C for 1 h) or 10 μg/ml trypsin (Cooper Biomedical, Inc.; activated in 0.001 N HCl). After incubation for 30 min at room temperature, the reaction was terminated by adding 3.5 vol of the sample buffer for electrophoresis and boiling for 2 min. The samples were analyzed by 13.5% PAGE (Laemmli, 1970). Fluorescence images of the gel were detected with an ISIT video camera (Dage-MTI, Inc., Michigan City, IN), and recorded with a digital image processor. The distribution of fluorescence among heavy and light chains was estimated by integrating the intensities within the bands and subtracting out the background.

Assembly of myosin was measured by right angle light scattering. Myosin in a buffer of 500 mM KCl, 0.1 mM EDTA, 10 mM Hepes, pH 7.5, was diluted 15–60 times with an assembly buffer containing 150 mM KCl, 10 mM $MgCl_2$, 1 mM EGTA, 0.1 mM DTT, 10 mM Hepes, pH 7.5, at room temperature. Scattered light intensities were measured with a Perkin-Elmer LS-3 spectrofluorimeter at a wavelength of 340 nm. Intensities of unpolymerized myosin at an identical concentration was subtracted from the values. Sensitivity of myosin filaments to ATP was determined by adding 100 mM ATP in the assembly buffer, to a final concentration of 5 mM, to preassembled myosin.

$K^+$-EDTA and $Ca^{2+}$-ATPase activities were measured at 36°C according to Pollard (1982), in a buffer of 500 mM KCl, 2 mM ATP, 50 mM Hepes, pH 7.5, and either 1 mM EDTA or 5 mM $CaCl_2$. $Mg^{2+}$-ATPases were assayed in a buffer of 50 mM KCl, 10 mM $MgCl_2$, 0.5 mM EGTA, 0.5 mM DTT, 2 mM ATP, 20 mM Pipes, pH 7.0.

### Cell Culture, Microinjection, and Microscopy

Swiss 3T3 cells were cultured and microinjected as described previously (Wang, 1987). A small volume of myosin at a relatively high concentration (5–9 mg/ml) was microinjected, in order to minimize cellular damage caused by the high salt in the injection buffer. The volume injected was far below the normal limit of needle microinjection (5–10% cell volume). Injected cells were incubated for 2–6 h to allow complete recovery. Immunofluorescence was performed as described previously (McKenna and Wang, 1986), using antibodies against platelet myosin.

All observations were made with a Carl Zeiss Inc. (Thornwood, NY) IM35 or an IM microscope, equipped with a 100× neofluar objective, NA 1.30. Living cells were maintained on the stage as described in McKenna and Wang (1989). Fluorescence images were detected with an ISIT video camera, and processed by frame averaging and background subtraction with a digital image processor (Meigs and Wang, 1986). Most sequences were recorded every 2–5 min, in order to minimize any light-induced damage to the cell. No damage was detected with either phase or fluorescence optics through the course of observation (up to 1 h). Images were photographed off a 9-in video monitor (model SNA-9C; Conrac Corp., Covina, CA; Wang, 1989), on Kodak Tri-X film and developed in Diafine. One sequence (Fig. 8) was processed by sharpening with a band-pass convolution filter before photography.

Dynamics of myosin filaments were observed by displaying a sequence of images in rapid succession. This greatly facilitated the identification of specific myosin-containing beads through a sequence, and the determination of the paths of movement. The coordinates of beads at different time points were then obtained with a graphics tablet, from which the speed was calculated.

## Results

### Characterization of Fluorescently Labeled Myosin

Myosin, containing unphosphorylated 20-kD light chain, was prepared from turkey gizzards and labeled with tetramethylrhodamine iodoacetamide, a reagent directed toward the cysteine sulfhydryl group. Bound fluorophores were distributed ~40% on the heavy chain and ~60% on the 17-kD light chain (Fig. 1). Furthermore, the fluorophore was located primarily at the 150-kD (tail plus the COOH-terminal region of S1 head; Marianne-Pèpin et al., 1983) and the 68-kD (S2 plus the COOH-terminal region of S1 head) fragments after trypsin digestion, and at the 95-kD (S1 head) and the 25-kD (COOH-terminal region of S1 head; Nath et al., 1986) fragments after papain digestion (Fig. 1). These results indicate unequivocally that the primary site of labeling on the heavy chain was the SH-C group, which corresponds to the SH-1 in skeletal muscle myosin (Nath et al., 1986).

The assembly of labeled myosin was measured with right angle light scattering. As shown in Fig. 2, labeled and unlabeled myosins followed an identical curve in the absence of ATP. However, when 5 mM ATP was added to the solution of myosin filaments, unlabeled myosin showed a >90% decrease in light scattering as a result of the 6–10 S conformational change (Suzuki et al., 1978), whereas labeled myosin showed a smaller, 40–50% decrease. Fluorescent labeling also induced a 30% decrease in the $K^+$-EDTA ATPase, a 14% activation of the $Ca^{2+}$-ATPase, and a fivefold increase in the $Mg^{2+}$-ATPase in the absence of actin filaments (Table I). Although the actin-activated $Mg^{2+}$-ATPase was three times higher than that with unlabeled, unphosphorylated myosin, the degree of activation by actin filaments was reduced for the fluorescent myosin. These observations were again consistent with the labeling of the SH-C group (Onishi, 1985; Nath et al., 1986).

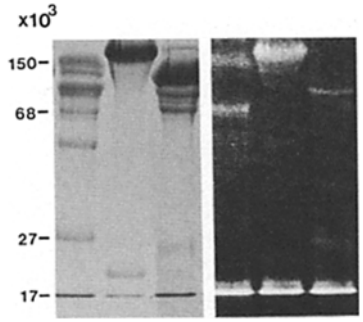


*Figure 1.* SDS-PAGE of fluorescently labeled myosin (*middle lanes*), and its proteolytic fragments created by trypsin (*left lanes*) and papain (*right lanes*). The left panel shows the pattern of Coomassie blue staining and the right panel shows the fluorescence. Approximate molecular weights are indicated on the left ($\times 10^3$).

## *Incorporation of Fluorescently Labeled Myosin into Living Fibroblasts*

The distribution of fluorescent myosin reached a steady state within 2 h of microinjection. Properly injected cells at this time showed no detectable change in morphology or behavior as compared to uninjected cells. Myosin-containing structures appeared to consist of beads of various intensities (Fig. 3). Well-resolved beads often showed an elongated or filamentous morphology (Fig. 3, *arrowhead*). The longer dimension of these beads had an apparent average length of 0.73 $\mu$m ($\pm$0.15 SD, $n$ = 79). When cells were processed for indirect immunofluorescence for myosin, similar structures were observed in both injected and uninjected cells (not shown). Moreover, the image of microinjected myosin was similar to that of myosin immunofluorescence when the two were compared using different fluorophores (Fig. 4). These results suggest that fluorescent myosin revealed normal, physiological structures.

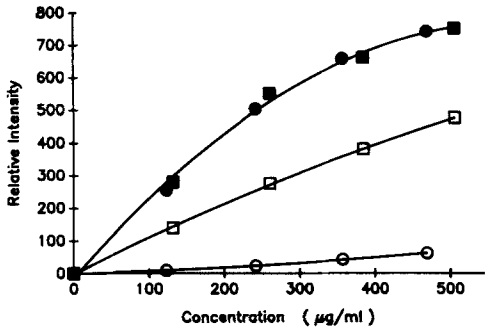


*Figure 2.* Assembly and ATP sensitivity of myosin filaments as a function of concentration. Myosin filaments were detected by right angle light scattering at 340 nm. Fluorescently labeled (■, □) or unlabeled (●, ○) myosin was assembled in an assembly buffer as described in Materials and Methods, and the steady-state intensities measured (■, ●). ATP was then added to the sample and the steady-state intensities measured again (□, ○). Labeled myosin shows normal assembly in the absence of ATP but a reduced sensitivity to ATP. The flattening of the upper curve at high concentrations was probably due to the inner filter effect since a similar flattening was observed with an increasing concentration of polystyrene beads.

*Table I. Effects of Fluorescent Labeling on Gizzard Myosin ATPases*

| Condition | Unlabeled | Tetramethylrhodamine iodoacetamide labeled | Labeled/unlabeled |
|---|---|---|---|
| | | | % |
| $K^+$-EDTA | 983 | 692 | 70 |
| $Ca^{2+}$ | 564 | 644 | 114 |
| $Mg^{2+}$ | 6.9 | 35.4 | 513 |
| $Mg^{2+}$-actin activated* | 14.4 | 42.8 | 297 |

All activities were measured at 36°C. All activities are expressed in units of nmol/min per mg.
* Measured in the presence of 0.53 mg/ml F-actin.

The myosin beads were either absent or present at a low density within the lamellipodia (Fig. 3, *small arrows*; and Fig. 5, *a* and *b*, see arrows in *b*); they were present at a high density throughout other regions of the cytoplasm. Several forms of arrangement were observed. Beads within or immediately behind the lamellipodia usually showed little organization, although they were often present in groups (Fig. 3, *small arrows*). Further behind the lamellipodia, the beads were arranged into linear structures, ranging from straight prominent fibers (Fig. 4, *short arrows*), which corresponded to alpha actinin-containing stress fibers (Fig. 5), to curved fine fibers or arrays (Figs. 3, 5, *c* and *d*, and 7), which were difficult to detect with microinjected fluorescent alpha actinin (Fig. 5, *c* and 5 *d*, note arrows in *c*). Sometimes the beads also formed a network-like pattern (Fig. 4, *long arrows*). Individual beads were more easily resolved along fine arrays (e.g., Fig. 3) than along stress fibers, showing an average spacing of 1.10 $\mu$m ($\pm$ 0.25 SD, $n$ = 82).

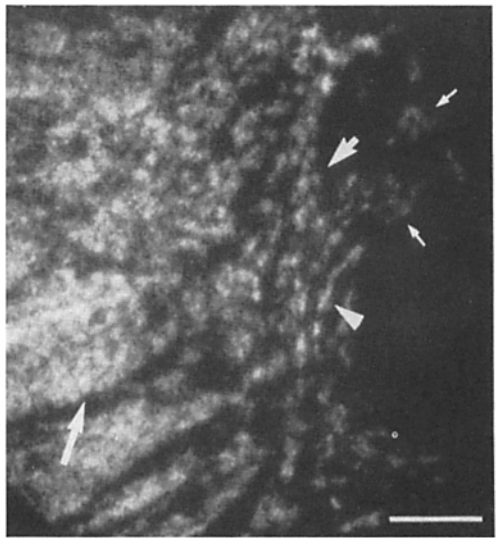

*Figure 3.* A living 3T3 cell microinjected with fluorescently labeled myosin, showing clearly resolved beads near the edge of the cell. Many beads appear elongated or filamentous (*arrowhead*). Near a lamellipodium, myosin beads are sparse, indistinct, and apparently poorly organized (*small arrows*). Further behind the lamellipodium, the beads are arranged along curved fibers that often seem to cross or merge with each other (*medium arrow*). The fibers appear tightly packed and laterally associated in a more central area (*large arrow*). A time-lapse sequence of the lamellipodial area is shown in Fig. 6. Bar, 5 $\mu$m.

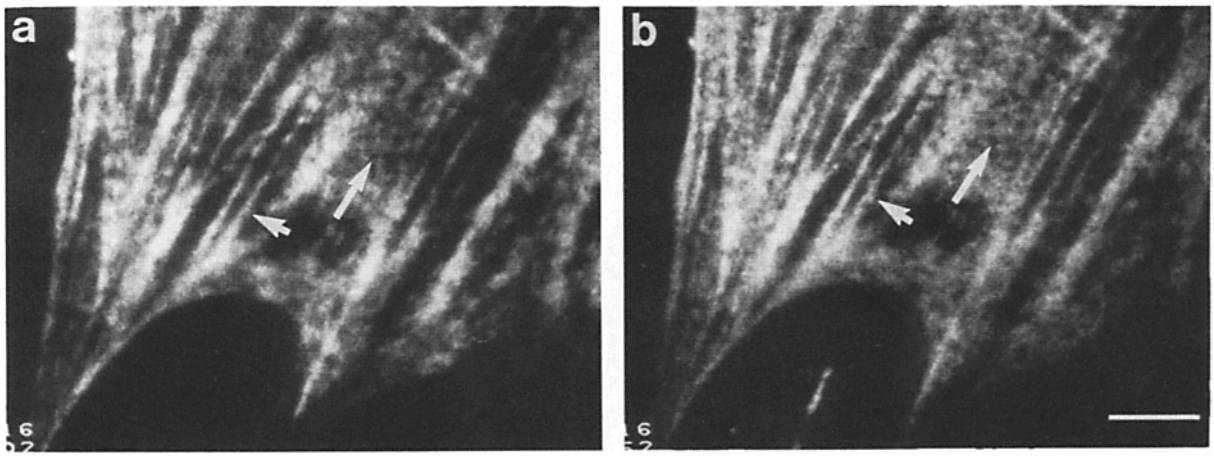


*Figure 4.* Comparison of microinjected myosin (*a*) and immunofluorescence of myosin (*b*). 3T3 cells were microinjected with tetramethylrhodamine-labeled myosin, incubated for 2 h, and processed for indirect immunofluorescence using fluorescein-labeled secondary antibodies. Filter sets selective for either rhodamine or fluorescein were used for the detection of images. A close correlation between the two fluorophores is observed. Myosin beads are arranged into both straight, well-defined stress fibers (*short arrows*) and network-like structures (*long arrows*). Bar, 5 μm.

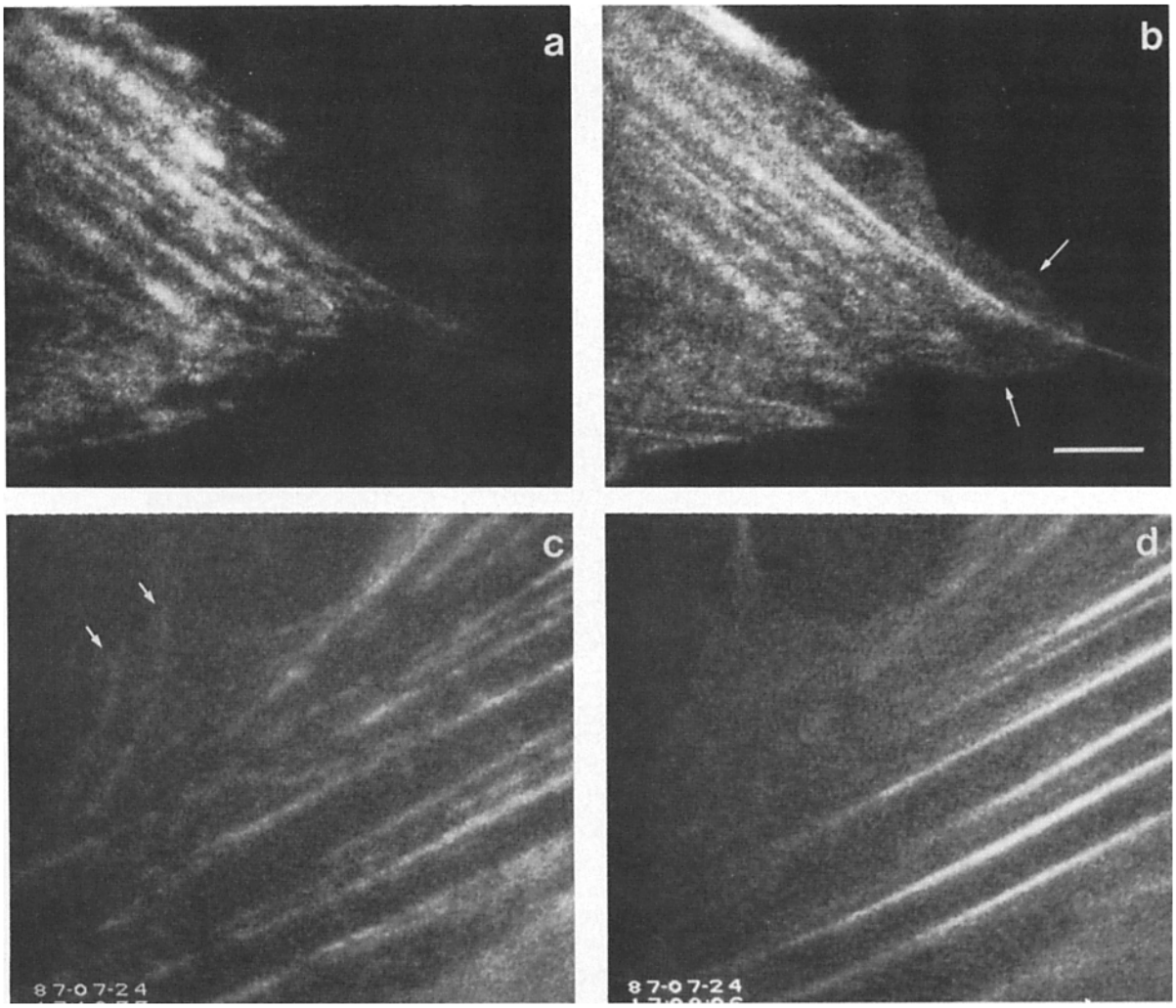


*Figure 5.* Comparison of the distributions of microinjected tetramethylrhodamine-labeled myosin (*a* and *c*) and microinjected fluorescein-labeled alpha actinin (*b* and *d*) in single living 3T3 cells. The first pair (*a* and *b*) show two neighboring lamellipodia that contain diffuse alpha actinin but little myosin (*arrows*). Most stress fibers, on the other hand, contain both alpha actinin and myosin in a punctate pattern. In the second pair (*c* and *d*), punctate myosin (*c*) and apparently continuous alpha actinin (*d*) are observed along stress fibers. Some fine linear structures near the edge of the cell contain punctates of myosin (*c*, *arrows*), but are undetectable with alpha actinin (*d*). Bar, 5 μm.

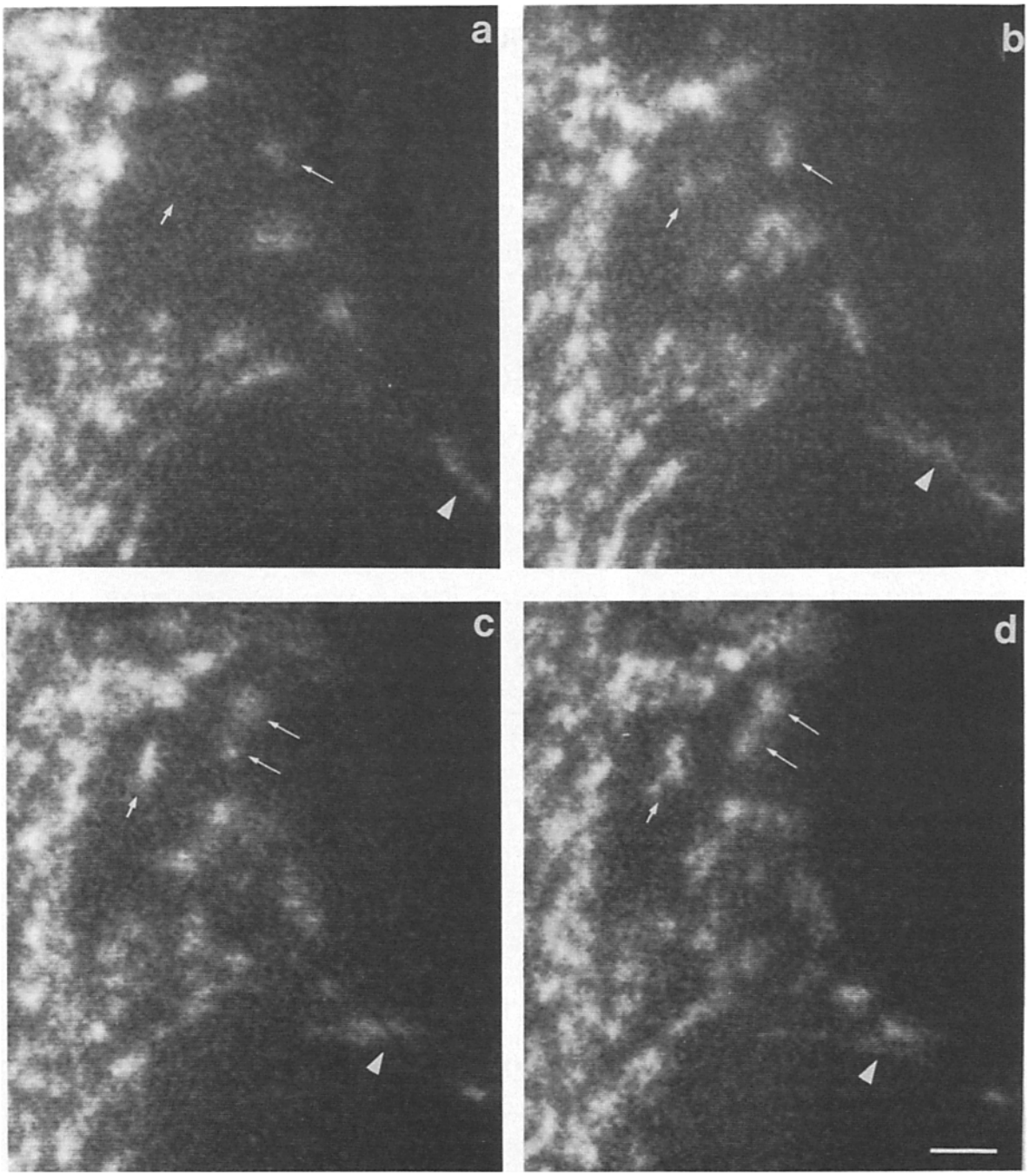


*Figure 6.* Formation of new myosin beads in a 3T3 cell microinjected with fluorescently labeled myosin. Images were recorded at 0 (*a*), 6 (*b*), 10 (*c*), and 13 min (*d*). Lamellipodium is located to the lower right. A bead forms de novo (*short arrows*), and later becomes elongated and appears to break into multiple beads (*d*). A group of beads originate near the lower right corner and subsequently move away from the lamellipodium, showing an increase in both size and intensity (*arrowheads*). The bead indicated by long arrows also becomes larger (*b*) before splitting into two beads (*c* and *d*). At this magnification, the more diffuse beads often seem to be comprised of smaller substructures. See Fig. 3 for a low magnification view of this cell. Bar, 2 μm.

### *Dynamics of Myosin Beads*

Time-lapse recording was used to detect changes in the organization of myosin beads. Observations were focused near existing lamellipodia, where poorly organized beads and beads arranged into fine linear structures were readily resolved and identified. Beads in this area fell within a common plane of focus due to the minimal thickness of the cytoplasm. Although similar activities appeared to occur along stress fibers, individual beads along stress fibers were often more difficult to identify with confidence over time. To simplify the interpretation of myosin translocation, observations were made only with cells showing no clear locomotion or retraction.

We have detected a continuous assembly of myosin beads within and immediately behind lamellipodia (Fig. 6). The

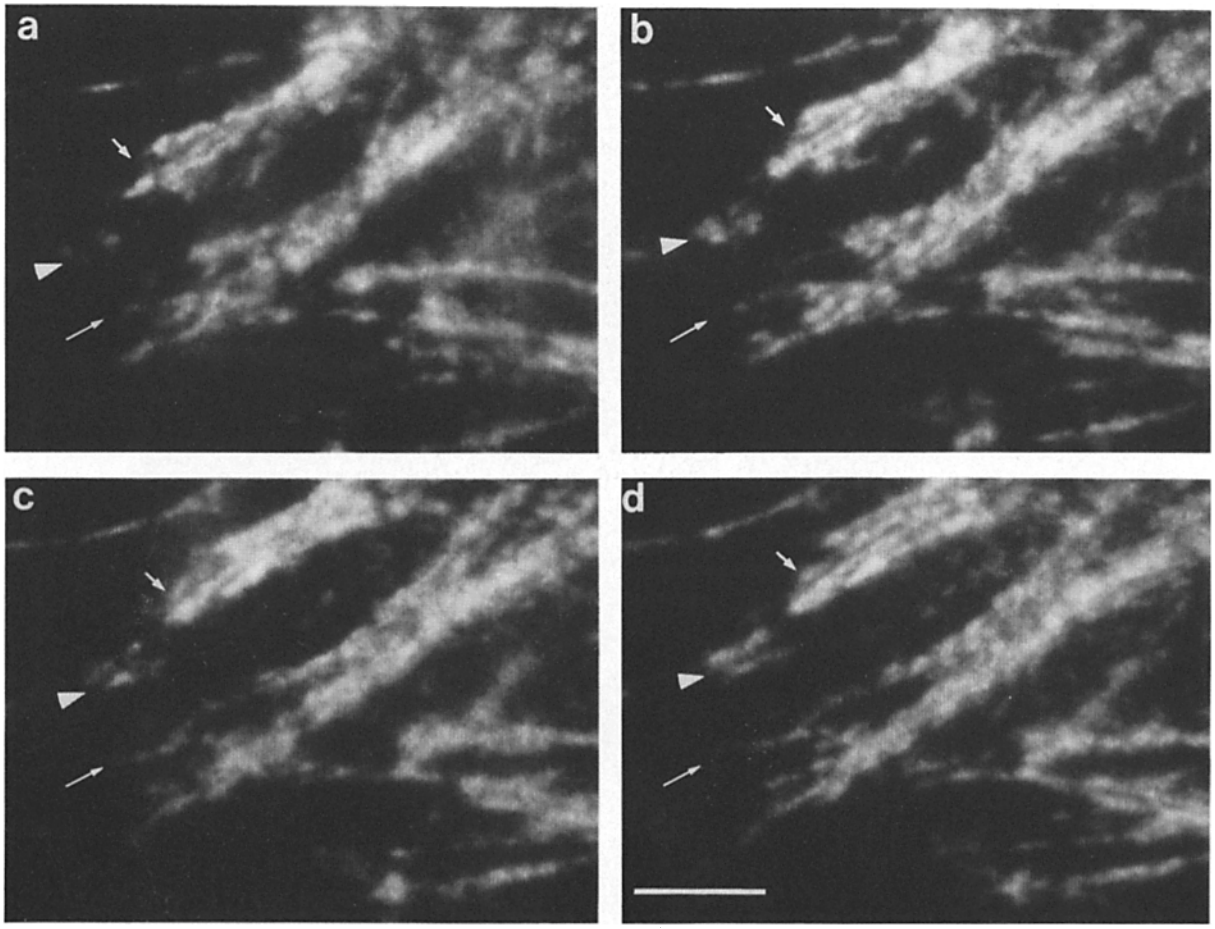


*Figure 7.* Formation and organization of new myosin beads near existing fine fibers in a cell microinjected with fluorescently labeled myosin. Images were recorded at 0 (*a*), 5 (*b*), 11 (*c*), and 14 min (*d*). The micrographs were cropped to show exactly the same area. Lamellipodium is located toward the lower left. A group of beads develop in size and become linearly organized, while moving away from the left edge of the photograph (*arrowheads*). Formation of new beads and reorganization are also observed in the area indicated by short arrows. Several new beads become organized into a linear array continuous with existing fibers (*long arrows*). Movement of these beads can be perceived based on the increasing distances from the left and/or bottom edges of the photograph. Bar, 5 μm.

assembly took place in both regions with no apparent organization of beads (Fig. 6), and regions containing linear arrays (Figs. 7 and 8). Many nascent beads appeared to assemble de novo; i.e., without a detectable precursor (Fig. 6, *short arrows*). However, frequently one bead structure gave rise to multiple beads (Fig. 6, *long arrows*), as if it contained or generated multiple nucleation sites.

By comparing fluorescence images of the same cell recorded at different time points, it was also clear that existing beads underwent constant changes in distribution (Figs. 7 and 8). Observations of such time-lapse images in rapid succession allowed us to identify specific myosin-containing beads in different images, and to conclude that the change in distribution is due primarily to the movement of beads toward the center of the cell, rather than the continuous assembly and disassembly of beads. Although it is more difficult to perceive such centripetal movement with stationary micrographs, the changes in location were evident based on changes in their distances from the edge of the micrograph or from reference points (Figs. 7, *arrowheads*, 8, *short arrows*, and 9). Movement in the opposite direction, toward the edge of the cell, was rarely observed (2 out of 30 cells recorded showed a localized region of forward movement). The movement was often accompanied by the organization or incorporation of beads into linear arrays (Figs. 7 and 8, *long arrows*). Similar movements were observed for both unorganized beads and beads already incorporated into linear structures. The movement would take different directions away from the lamellipodia (Fig. 9), and proceed with no detectable reversal in direction during the course of observation. Furthermore, neighboring beads usually moved in the same direction at a similar speed, as if there were discrete domains or tracks (Fig. 9). By tracing the locations of 45 beads over periods of 5–20 min, we have obtained an average speed of 0.18 μm/min (SD = 0.09 μm/min). It should be emphasized that the movement of beads occurred relative to the substrate, and cannot be explained by the net movement or retraction of the cell.

## Discussion

Smooth muscle myosin was used in the present study because of its close similarities to nonmuscle myosin in both self-assembly properties and regulation of the actin-activated ATPase (Scholey et al., 1982; Kendrick-Jones et al., 1982). A tetramethylrhodamine conjugate was prepared and then

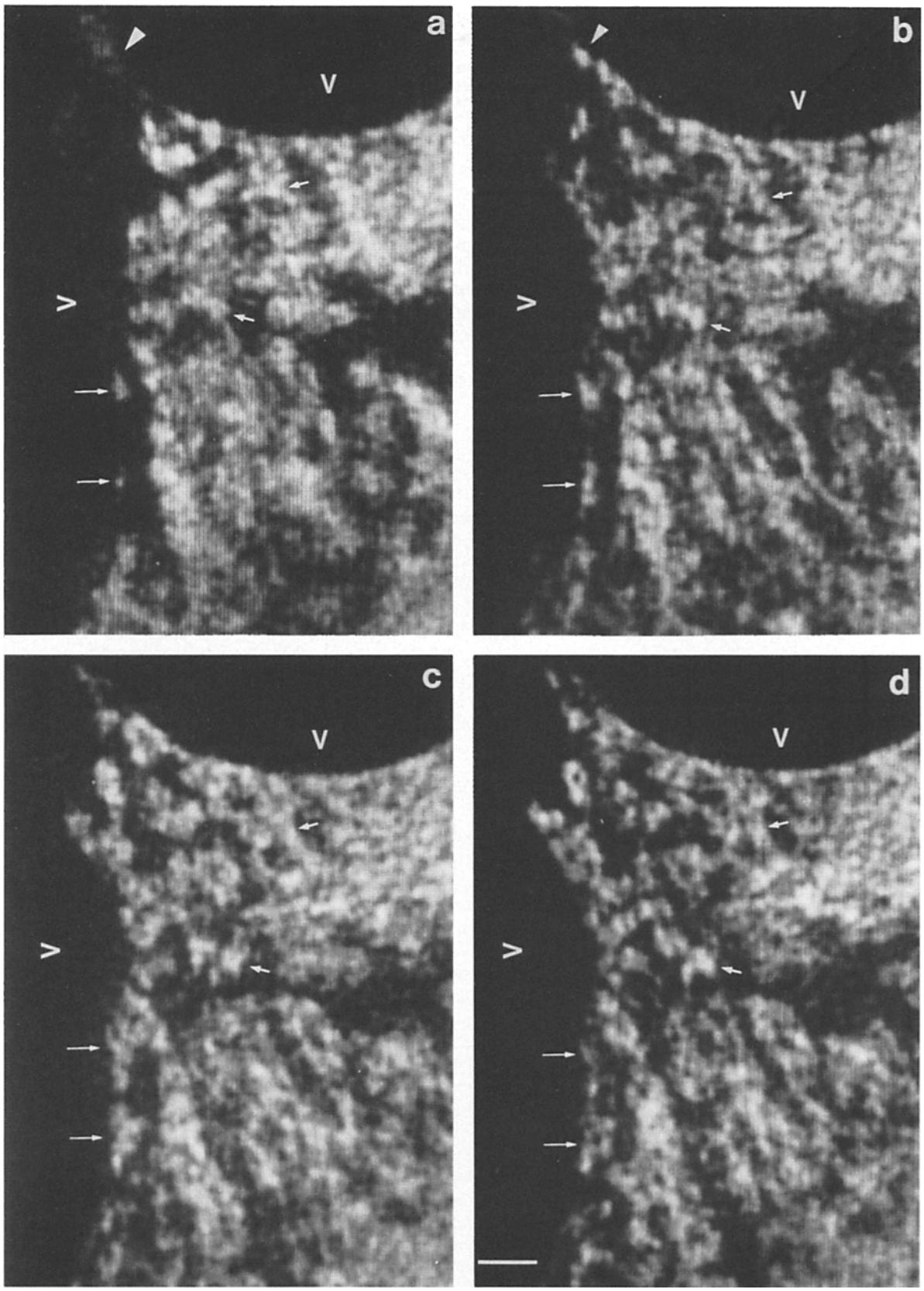


*Figure 8.* Formation, movement, and organization of myosin beads in a 3T3 cell microinjected with fluorescent myosin. Images were recorded at 0 (*a*), 5 (*b*), 10 (*c*), and 13 min (*d*). Fixed reference points are marked (*V*). (*a*) Faint, diffuse fluorescence is present in a lamellipodium (*arrowhead*). New beads subsequently appear in this area (*b*, *arrowhead*). Movement of two beads (*short arrows*) is detectable based on changes in their positions relative to the reference points. Long arrows point to a region where new beads are generated and organized into linear arrays. Bar, 2 μm.

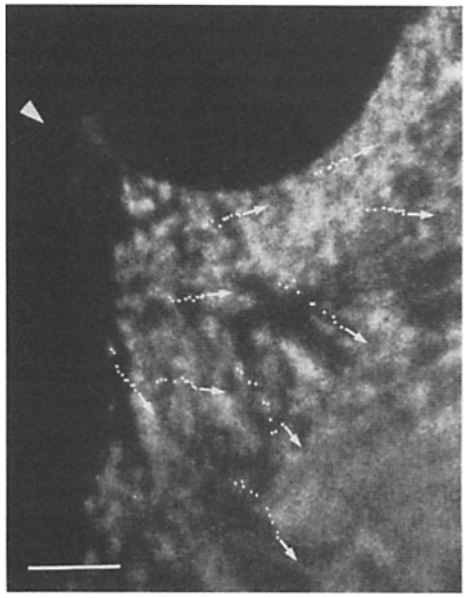

*Figure 9.* A lower magnification view of the cell in Fig. 8, showing changes in the location of 9 individual myosin beads over a period of 21 min. Their positions, measured at 2–3-min intervals, are indicated as small white dots. Arrows indicate the directions of net translocation over the period of observation. Although beads in general move away from the lamellipodium region (*arrowhead*), they can nevertheless move in different directions. There appear to be discrete domains: beads near the upper edge of the cell move toward the upper right, whereas those in the lower half move toward the lower right. Bar, 5 μm.

microinjected into living fibroblasts to reveal the distribution of cytoplasmic myosin-containing structures. This approach, fluorescent analogue cytochemistry, has been applied previously to examine the reorganization of actin, alpha actinin, and vinculin in living fibroblasts (reviewed by Wang et al., 1981; Wang, 1989; Jockusch et al., 1986). It has also been used recently to demonstrate the incorporation of exogenous myosin into living myotubes and fibroblasts (Johnson et al., 1988; DeBiasio et al., 1988), and the colocalization of exogenous myosin light chains with endogenous myosin-containing structures (Mittal et al., 1987).

Proteolytic analyses indicated that the tetramethylrhodamine groups were associated primarily with the SH-B of the 17-kD light chain, and the SH-C group of the heavy chain near the COOH terminus of the S1 head (Nath et al., 1986). While important characteristics of myosin, including self-assembly and actin-activated ATPase activities, were preserved qualitatively after fluorescent labeling, there were quantitative changes similar to those induced by other sulfhydryl reacting agents (Onishi, 1985; Chandra et al., 1985; Nath et al., 1986). For example, the actin-activated ATPase activity of labeled myosin was different from that of unlabeled, unphosphorylated myosin, but was more similar to that of phosphorylated myosin which is probably the predominant form in filamentous structures (Suzuki et al., 1978). In addition, the partial inhibition of ATP-induced disassembly suggests that the labeled myosin may exist more preferentially in the assembled state in the cell, and thus may not reveal the true distribution of endogenous myosin molecules between the assembled and unassembled states. Taken together, these results suggest that the microinjection may induce subtle effects equivalent to an increase in the overall extent of phosphorylation (the extent of phosphorylation of myosin appears high in normal cultured fibroblasts; Lamb et al., 1988). However, the fluorescent analogue should function as a useful probe for myosin filaments and may even facilitate their detection.

The cellular effects of labeled myosin should also be minimized by the limited amount introduced into living cells. We may assume that a maximum of 2% cell volume of myosin at 8 mg/ml was microinjected. If a cell contains 1 mg/ml myosin (Clarke and Spudich, 1977; Höner et al., 1988), the amount of injected analogue would correspond to no more than 16% of the endogenous counterpart. The similarities between the distributions of myosin in injected and uninjected cells, and between the distributions of fluorescent myosin and total myosin, indicated that the analogue probably co-assembled with endogenous myosin into physiological structures. In addition, it is likely that the observed movement of myosin beads represents physiological activities of myosin molecules. If this were an artifact induced by the microinjection of analogues, one would expect changes to be observed in cellular morphology, behavior, or distribution of myosin.

It appeared that most myosin-containing structures in cultured fibroblasts consist of small beads. The average length, 0.7 μm, of well-defined beads was similar to that of the "rods" observed in the slime mold *Dictyostelium* (Yumura and Fukui, 1985). Immunoelectron microscopy by Langanger et al. (1986) further demonstrated that the beads along stress fibers are bipolar myosin filaments. In the present study, beads were found along stress fibers and fine linear arrays, and as poorly organized structures within or near the lamellipodia. Fine fibers and networks of beads have previously been reported in cultured human and chick fibroblasts (Zigmond et al., 1979; Langanger et al., 1986). It is possible that these different organizational forms may represent similar linear structures with different degrees of lateral association.

So far little is known about the poorly organized myosin beads near the lamellipodia. DeBiasio et al. (1988) recently reported that myosin beads were undetectable in lamellipodia during the initial protrusion, and became detectable only after the initial protrusion had stopped. Our time-lapse analyses suggested that the appearance of beads in lamellipodia is a result of de novo assembly, rather than a result of centrifugal movement of preexisting beads into the lamellipodia. The newly formed beads then move away from the edge of the cell, and become organized into linear structures. Similar centripetal movement of beads was also observed along existing linear structures. These results suggest that there may be a continuous cycling of myosin molecules between assembled and unassembled forms. One possible model is that the lamellipodia represent an area of active assembly of myosin filaments. In order for the cell to maintain a steady-state number and distribution of myosin filaments, sites of disassembly, which may be located in the perinuclear area or the trailing end, must also exist. If this model is correct, myosin molecules would undergo continuous cycles between the backward moving, filamentous form, and the forward diffusing, monomeric form. However, although such a cycling model appears attractive, we are presently unable to exclude the possibility that assembly occurs in areas outside lamellipo-

dia, or to identify the sites of disassembly due to the thickness of cytoplasm in regions far behind the lamellipodium.

How do myosin beads move in the cell? The simplest mechanism is through interactions with actin filaments. However, a centripetal movement as observed here would require interactions of myosin selectively with actin filaments of a uniform polarity, with their barbed ends pointing away from the edge of the cell. This appears difficult to reconcile with the opposite polarity of actin filaments inside lamellipodia (Small et al., 1978), and the mixed polarity of actin filaments in other regions of the cytoplasm (Begg et al., 1978). Alternatively, myosin and cortical actin may move as a complex, as a result of a global balanace of forces among different regions of the cortex. An important question is therefore whether the movement of myosin is coupled to the movement of actin filaments. We have previously observed a centripetal flux of actin subunits within the lamellipodia (Wang, 1985; see also Fisher et al., 1988) and along stress fibers near the trailing end of the cell (McKenna and Wang, 1986). The movement of actin-containing "arcs" has also been reported in newly spread cells (Heath, 1983). However, it is not clear if a similar movement takes place in the absence of arcs in the area immediately behind the lamellipodia, where movement of myosin beads was most clearly observed.

The functional role of the movement of myosin beads is unclear. Since disruptions of myosin molecules by either genetic manipulations (De Lozanne and Spudich, 1987; Knecht and Loomis, 1987) or microinjections of antibodies against myosin (Höner et al., 1988) failed to inhibit cell locomotion, the movement is unlikely to be required for cytoplasmic protrusion. However, injection of antibodies did cause a dramatic change in cell shape and induce the formation of lamellipodia over a large area of the cell, suggesting that the polarity of the cell may have been disrupted. The movement of myosin may also play an important role in surface capping and in the formation of the contractile ring during cytokinesis (Bray and White, 1988). In addition, if myosin is involved in the transport of organelles during cell locomotion, its backward movement may be coupled to the forward movement of the cytoplasmic matrix or organelles.

The authors would like to thank Dr. Ira Herman, Tufts University Medical School, for supplying antibodies against platelet myosin.

Our studies were supported by grants from the Muscular Dystrophy Association, National Institutes of Health (GM-32476), and National Science Foundation (DCB-8796359).

Received for publication 11 January 1989 and in revised form 10 March 1989.

## References

Begg, D. A., R. Rodewald, and L. I. Rebhun. 1978. The visualization of actin filament polarity in thin sections. Evidence for the uniform polarity of membrane-associated filaments. *J. Cell Biol.* 79:846–852.

Bourguignon, L. Y. W., and S. J. Singer. 1977. Transmembrane interactions and the mechanism of capping of surface receptors by their specific ligands. *Proc. Natl. Acad. Sci. USA.* 74:5031–5035.

Bray, D., and J. G. White. 1988. Cortical flow in animal cells. *Science (Wash. DC).* 239:883–888.

Chandra, T. S., N. Nath, H. Suzuki, and J. C. Seidel. 1985. Modification of thios of gizzard myosin alters ATPase activity, stability of myosin filaments, and the 6–10S conformational transition. *J. Biol. Chem.* 260:202–207.

Clarke, M., and J. A. Spudich. 1977. Nonmuscle contractile proteins: the role of actin and myosin in cell motility and shape determination. *Annu. Rev. Biochem.* 46:797–822.

DeBiasio, R. L., L.-L. Wang, G. W. Fisher, and D. L. Taylor. 1988. The dynamic distribution of fluorescent analogues of actin and myosin in protrusions at the leading edge of migrating Swiss 3T3 fibroblasts. *J. Cell Biol.* 107:2631–2645.

De Lozanne, A., and J. A. Spudich. 1987. Disruption of the *Dictyostelium* myosin heavy chain gene by homologous recombination. *Science (Wash. DC).* 236:1086–1091.

Fisher, G. W., P. A. Conrad, R. L. DeBiasio, and D. L. Taylor. 1988. Centripetal transport of cytoplasm, actin, and the cell surface in lamellipodia of fibroblasts. *Cell Motil. Cytoskeleton.* 11:235–247.

Fujiwara, K., and T. D. Pollard. 1976. Fluorescent antibody localization of myosin in the cytoplasm, cleavage furrow, and mitotic spindle of human cells. *J. Cell Biol.* 71:848–875.

Heath, J. P. 1983. Behavior and structure of the leading lamella in moving fibroblasts. I. Occurrence and centripetal movement of arc-shaped microfilament bundles beneath the dorsal cell surface. *J. Cell Sci.* 60:331–354.

Höner, B., S. Citi, J. Kendrick-Jones, and B. M. Jockusch. 1988. Modulation of cellular morphology and locomotory activity by antibodies against myosin. *J. Cell Biol.* 107:2181–2189.

Ikebe, M., and D. Hartshorne. 1985. Effects of $Ca^{2+}$ on the conformation and enzymatic activity of smooth muscle myosin. *J. Biol. Chem.* 260:13146–13153.

Jockusch, B. M., A. Fuchtbauer, C. Wiegand, and B. Honer. 1986. Probing the cytoskeleton by microinjection. *In* Cell and Molecular Biology of the Cytoskeleton. J. W. Shay, editor. Plenum Publishing Corp., New York. 1–40.

Johnson, C. S., N. M. McKenna, and Y.-L. Wang. 1988. Association of microinjected myosin and its subfragments with myofibrils in living muscle cells. *J. Cell Biol.* 107:2213–2221.

Kendrick-Jones, J., W. Z. Cande, P. J. Tooth, R. C. Smith, and J. M. Scholey. 1983. Studies on the effect of phosphorylation of the 20,000 $M_r$ light chain of vertebrate smooth muscle myosin. *J. Mol. Biol.* 165:139–162.

Kendrick-Jones, J., K. A. Taylor, and J. M. Scholey. 1982. Phosphorylation of nonmuscle myosin and stabilization of thick filament structure. *Methods Enzymol.* 85:364–370.

Knecht, D. A., and W. F. Loomis. 1987. Antisense RNA inactivation of myosin heavy chain gene expression in *Dictyostelium discoideum. Science (Wash. DC).* 236:1081–1086.

Korn, E. D., and J. A. Hammer, III. 1988. Myosins of nonmuscle cells. *Annu. Rev. Biophys. Biophys. Chem.* 17:23–45.

Laemmli, U. K. 1970. Cleavage of structural proteins during the assembly of the head of bacteriophage T4. *Nature (Lond.).* 227:680–685.

Lamb, N. J. C., A. Fernandez, M. A. Conti, R. Adelstein, D. B. Glass, W. J. Welch, and J. R. Feramisco. 1988. Regulation of actin microfilament integrity in living nonmuscle cells by the cAMP-dependent protein kinase and the myosin light chain kinase. *J. Cell Biol.* 106:1955–1971.

Langanger, G., M. Moeremans, G. Daneels, A. Sobieszek, M. De Branbander, and J. De Mey. 1986. The molecular organization of myosin in stress fibers of cultured cells. *J. Cell Biol.* 102:200–209.

Marianne-Pèpin, T., D. Mornet, E. Audemard, and R. Kassab. 1983. Structural and actin-binding properties of the trypsin-produced HMM and S1 from gizzard smooth muscle myosin. *FEBS (Fed. Eur. Biochem. Soc.) Lett.* 159:211–216.

McKenna, N. M., and Y.-L. Wang. 1986. Possible translocation of actin and alpha-actinin along stress fibers. *Exp. Cell Res.* 167:95–105.

McKenna, N. M., and Y.-L. Wang. 1989. Culturing cells on the microscope stage. *Methods Cell Biol.* 29:195–205.

Meigs, J. B., and Y.-L. Wang. 1986. Reorganization of alpha-actinin and vinculin induced by a phorbol ester in living cells. *J. Cell Biol.* 102:1430–1438.

Mittal, B., J. M. Sanger, and J. W. Sanger. 1987. Visualization of myosin in living cells. *J. Cell Biol.* 105:1753–1760.

Nath, N., S. Nag, and J. C. Seidel. 1986. Localization of sites of reaction of *N*-ethylmaleimide in papain and chymotrypsin fragments of the gizzard myosin heavy chain. *Biochemistry.* 25:6169–6176.

Onishi, H. 1985. *N*-iodoacetyl-*N'*-(5-sulfo-1-naphthyl)ethylenediamine modification of myosin from chicken gizzard. *J. Biochem. (Tokyo).* 98:81–86.

Perrie, W. T., and S. V. Perry. 1970. An electrophoretic study of the low-molecular-weight components of myosin. *Biochem. J.* 119:31–38.

Pollard, T. D. 1982. Myosin purification and characterization. *Methods Cell. Biol.* 24:333–371.

Scholey, J. M., R. C. Smith, D. Drenckhahn, U. Groschel-Stewart, and J. Kendrick-Jones. 1982. Thymus myosin. Isolation and characterization of myosin from calf thymus and thymic lymphocytes and studies on the effect of phosphorylation of its $M_r$ = 20,000 light chain. *J. Biol. Chem.* 257:7737–7745.

Sheetz, M. P., and J. A. Spudich. 1983. Movement of myosin-coated fluorescent beads on actin cables in vitro. *Nature (Lond.).* 303:31–35.

Small, J. V., G. Isenberg, and J. E. Celis. 1978. Polarity of actin at the leading edge of cultured cells. *Nature (Lond.).* 272:638–639.

Suzuki, H., H. Onishi, K. Takahashi, and S. Watanabe. 1978. Structure and function of chicken gizzard myosin. *J. Biochem. (Tokyo).* 84:1529–1542.

Wang, Y.-L. 1985. Exchange of actin subunits at the leading edge of living fibroblasts: possible role of treadmilling. *J. Cell Biol.* 101:597–602.

Wang, Y.-L. 1987. Mobility of filamentous actin in living cytoplasm. *J. Cell Biol.* 105:2811–2816.

Wang, Y.-L. 1989. Fluorescent analog cytochemistry: tracing functional protein components in living cells. *Methods Cell Biol.* 29:1–12.

Wang, Y.-L., J. M. Heiple, and D. L. Taylor. 1981. Fluorescent analog cytochemistry of contractile proteins. *Methods Cell Biol.* 25:1–11.
Warrick, H. M., and J. A. Spudich. 1987. Myosin structure and function in cell motility. *Annu. Rev. Cell Biol.* 3:379–421.
Yumura, S., and Y. Fukui. 1985. Reversible cyclic AMP-dependent change in distribution of myosin thick filaments in *Dictyostelium*. *Nature (Lond.)*. 314:194–196.
Zigmond, S. H., J. J. Otto, and J. Bryan. 1979. Organization of myosin in a submembranous sheath in well-spread human fibroblasts. *Exp. Cell Res.* 119:205–219.